Journal of Atmospheric and Solar-Terrestrial Physics 70 (2008) 2014–2030

Contents lists available at ScienceDirect

Journal of Atmospheric and Solar-Terrestrial Physics

journal homepage: www.elsevier.com/locate/jastp

Long-term thermospheric neutral wind observations over the northern polar cap

Q. Wu [a,*], D. McEwen [b], W. Guo [b], R.J. Niciejewski [c], R.G. Roble [a], Y.-I. Won [d]

[a] High Altitude Observatory, National Center for Atmospheric Research, P. O. Box 3000, Boulder, CO 80307-3000, USA
[b] Department of Physics and Engineering Physics, University of Saskatchewan, 116 Science Place, Saskatoon, Saskatchewan, Canada S7N 5E2
[c] Space Physics Research Laboratory, The University of Michigan, 2455 Hayward Street, Ann Arbor, MI 48109-2143, USA
[d] RSIS, Goddard Earth Science DISC, NASA Goddard Space Flight Center, Mailstop 610.2, Greenbelt, MD 20771, USA

ARTICLE INFO

Article history:
Received 4 April 2008
Received in revised form
13 August 2008
Accepted 3 September 2008
Available online 27 September 2008

Keywords:
Thermospheric dynamics
Polar cap
Fabry–Perot interferometer
Solar effect

ABSTRACT

We study the solar dependence of the thermospheric dynamics based on more than 20 years Fabry–Perot interferometer O 6300 Å emission observation of polar cap thermospheric wind from three stations: Thule (76.53°N, 68.73°W, MLAT 86N), Eureka (80.06°N, 86.4°W, MLAT 89N), and Resolute (74.72°N, 94.98°W, MLAT 84N) in combination with the National Center for Atmospheric Research Thermosphere Ionosphere Electrodynamics General Circulation Model (NCAR-TIEGCM). All three stations showed a dominant diurnal oscillation in both the meridional and zonal components, which is a manifestation of anti-sunward thermospheric wind in the polar cap. The three-station observations and the TIEGCM simulation exhibit varying degree of correlations between the anti-sunward thermospheric wind and solar F10.7 index. The diurnal oscillation is stronger at Eureka (~150 m/s) than that at Resolute (~100 m/s) according to both observations and TIEGCM simulation. The semidiurnal oscillation is stronger at Resolute (~20 m/s) than that at Eureka based (~10 m/s) on data and model results. These results are consistent with a two-cell convection pattern in the polar cap thermospheric winds. The Thule results are less consistent between the model and observations. The simulated meridional wind diurnal and semidiurnal oscillations are stronger than those observed.

1. Introduction

The high-latitude thermospheric winds are affected by day–night pressure gradient, ion drag, and the Coriolis force. The day–night pressure gradient is related to the thermosphere day–night temperature difference, which is directly connected with solar activity. Ion convection is closely controlled by the cross-polar cap potential, which is affected by the magnetosphere–ionosphere coupling. Hence, the polar cap thermospheric winds tend to manifest both solar and geomagnetic activities. There have been numerous high-latitude thermospheric wind studies in the past (e.g. Killeen et al., 1995; Meriwether et al., 1988; McCormac and Smith, 1984).

What was lacking is a decadal scale long-term study of the solar dependence study at very high latitudes. Some past studies have examined solar dependence with shorter data sets. Won (1994) and Killeen et al. (1995) examined Thule, Greenland Fabry–Perot interferometer (FPI) O(*D*) 6300 Å nightglow neutral wind data from 1985 to 1989 to study the solar and geomagnetic dependence of the thermospheric neutral winds and temperature. They reported a strong correlation between the F10.7 index and thermospheric neutral winds. Even though the length of

* Corresponding author.
E-mail address: qwu@ucar.edu (Q. Wu).

1364-6826/$ - see front matter
doi:10.1016/j.jastp.2008.09.004

the data (4 years) is shorter than a solar cycle, the underlying fact is that a long-term data set is hard to obtain given the harsh condition in the polar region and the effort required operating an instrument on a long-term basis.

At somewhat lower latitudes, Aruliah et al. (1991, 1996) have analyzed the FPI thermospheric wind data from Kiruna, Sweden (67.8°N, 20.4°E, MLAT 65N) for solar and seasonal and geomagnetic dependences. Probably because the latitude is lower, the changes associated with the solar F10.7 index are much smaller than these observed at Thule by Killeen et al. (1995). At the vicinity of the Kiruna, Sweden, the EISCAT incoherent scatter radar (70°N, 19°E) has been operated over a long time. From the EISCAT radar measurement, one can deduce the thermospheric meridional winds. Using data from January 1984 to March 1995, Witasse et al. (1998) analyzed the solar and season dependence of the meridional winds. They extracted the diurnal and semidiurnal oscillations from the thermospheric winds and noted that the amplitude of the 24-h oscillation in the winter season increased with the solar F10.7 index.

There are reports on thermospheric wind observations at the South Pole, Antarctica, which is on edge of the polar cap (MLAT 75S) (Hernandez et al., 1990; Hernandez et al., 1991; Smith et al. 1994). Hernandez and Roble (2003) reported storm time observations over both South Pole and Arrival Heights (77.8°S, 166.66°E, MLAT 80S). Arrival Heights is a polar cap observatory. Comparisons between observations at Arrival Heights and the Thermosphere Ionosphere Mesosphere Electrodynamics General Circulation Model (NCAR-TIMEGCM) model run show mostly consistent anti-sunward wind patterns. There is no analysis of long-term trends in the Arrival Heights data yet.

Other Antarctic thermospheric wind observations were made on the edge of the polar cap or lower latitudes. For example, Conde and Dyson (1995) and Greet et al. (1999) reported thermospheric wind measurements from Mawson (67.6°S, 62.9°E, MLAT 70S) and Davis (68.6°S, 78.0°E, MLAT 74.5S), Antarctica. Long-term analysis on these data sets has not been reported yet.

Emmert et al. (2006a, b) examined the high-latitude thermospheric winds during geomagnetically quiet conditions. They examined thermospheric winds at various latitudes. In the northern high latitudes, they also analyzed the Thule thermospheric wind data. An increase in the thermospheric wind due to the solar activity was clearly demonstrated from the Thule data at all local times.

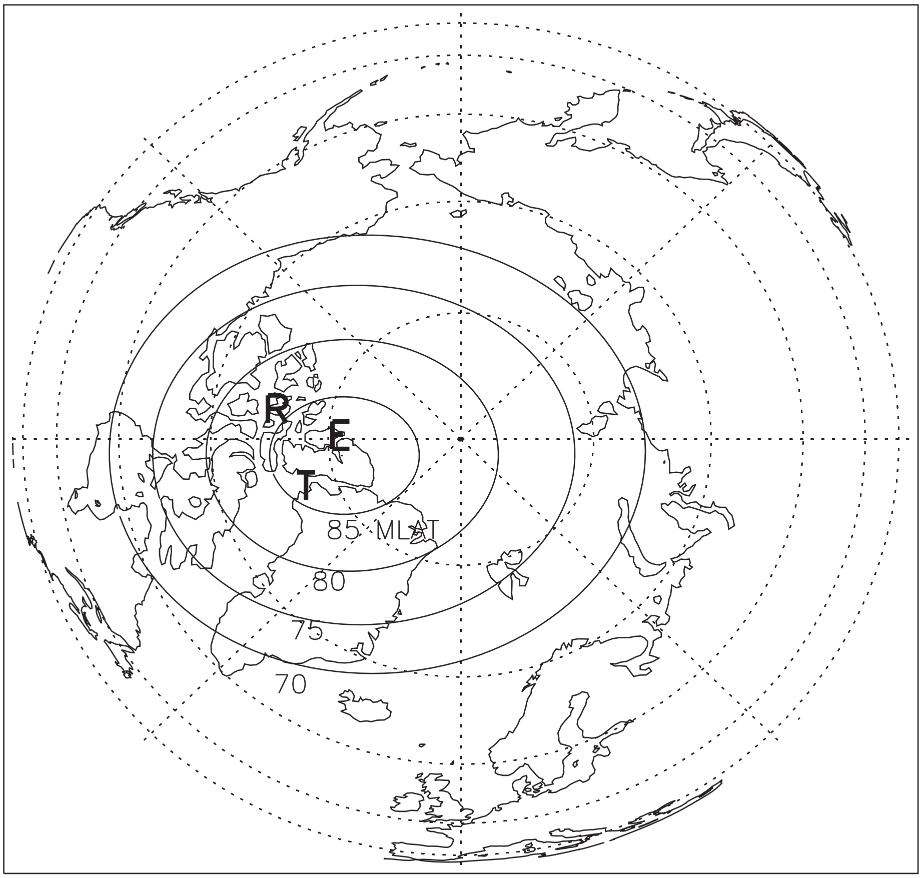

Fig. 1. Location of Thule, Eureka, and Resolute. The locations of the Thule (T), Eureka (E), and Resolute (R) are plotted. The magnetic latitudes from APL PACE program are also shown in the plot.

Satellite observations of the thermospheric winds have provided crucial information about the morphology of the polar cap convection in connection with the IMF and geomagnetic activity (Killeen et al., 1985; McCormac et al., 1985). However, because of the relatively short data set, it is not possible to examine the solar dependence based on those satellite observations.

The mechanism for the solar activity to affect the polar cap thermospheric neutral wind is the higher day–night thermosphere temperature gradient caused by high solar UV radiation flux. However, to obtain a more accurate assessment of the solar influence on the polar cap thermospheric neutral winds, a longer data set inside the polar cap is needed. This information will be invaluable to future aeronomy studies in the northern polar cap related to the Advanced Modular Incoherent Scatter Radar (AMISR) in Resolute, Canada. A longer data set will provide a baseline for polar cap thermospheric wind climatology.

The goal of this paper is to combine the Thule data set from 1980s used by Won (1994) and Killeen et al. (1995) with similar Eureka data from the 1990s and Resolute data from 2000s, to examine the climatology and, perhaps, morphology of the thermospheric neutral wind over the northern polar cap. The locations of the three stations are shown in Fig. 1. All three stations are located inside the polar cap, and Eureka has highest magnetic latitude, followed by Thule and Resolute according to the APL PACE corrected magnetic latitude calculation. The data set expands over 20 years and cover nearly two solar cycles with some data gaps. Fig. 2 shows the solar F10.7 index and FPI coverage. The blue is for Thule, red for Eureka, and green for Resolute. The coverage for 90/91 winter season was small and the Thule FPI had some instrument problems, hence, the data were not used in final analysis. While the combined data set is longer, the fact that data came from three different stations and instruments poses new challenges in data analysis and comparison. We are hampered somewhat by the fact that we do not have time overlap between these three observations. Nevertheless, the combined data can provide a new insight to the solar influence on the polar cap thermospheric neutral winds.

We focus on the long-term solar influence and avoid the geomagnetic effect, which can also enhance the wind. Another important factor is the interplanetary magnetic field (IMF) as demonstrated by Niciejewski et al. (1994). Both the geomagnetic and IMF effects are all related to the ion drift and beyond the scope of this paper. It will be necessary to include the ion drift data included in such analysis. There have been many past studies of high-latitude ion neutral interaction (e.g., Heelis et al., 2002; Thayer et al., 1995). The future Resolute AMISR will provide high-quality ion drift data and allow more comprehensive and systematic study of the subject.

The solar influence on the polar thermospheric wind is important to the understanding of solar effects on the thermosphere in general. We should expect a seasonal effect on the thermospheric winds as well. However, since

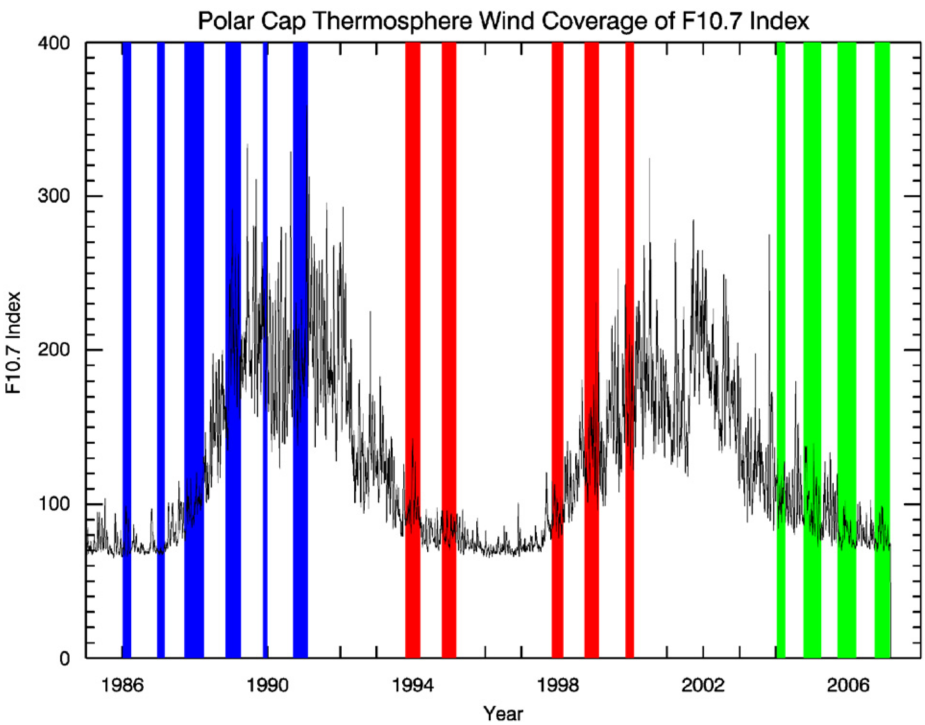

Fig. 2. Thermospheric wind and F10.7 index coverage. The time coverage from Thule (blue), Eureka (red), and Resolute (green) are shown with F10.7 index from 1985 to 2006.

most of the optical data were taken during long polar winter nights, these observations are not suitable for seasonal analysis. Therefore, more attention will be given to inter-annual variations induced possibly by the solar variations.

To provide a better interpretation for the observational results, we use the NCAR-TIEGCM 1.8 model (Richmond et al., 1992) to simulate the polar thermospheric winds for years when we have a good coverage during the December solstice. Model run results can help interpret inter-station differences due to magnetic latitudinal differences. More important, the TIEGCM may shed some light on the solar dependence of the high-latitude thermospheric winds. Conversely, comparison with observations can also help fine tuning of the model parameters.

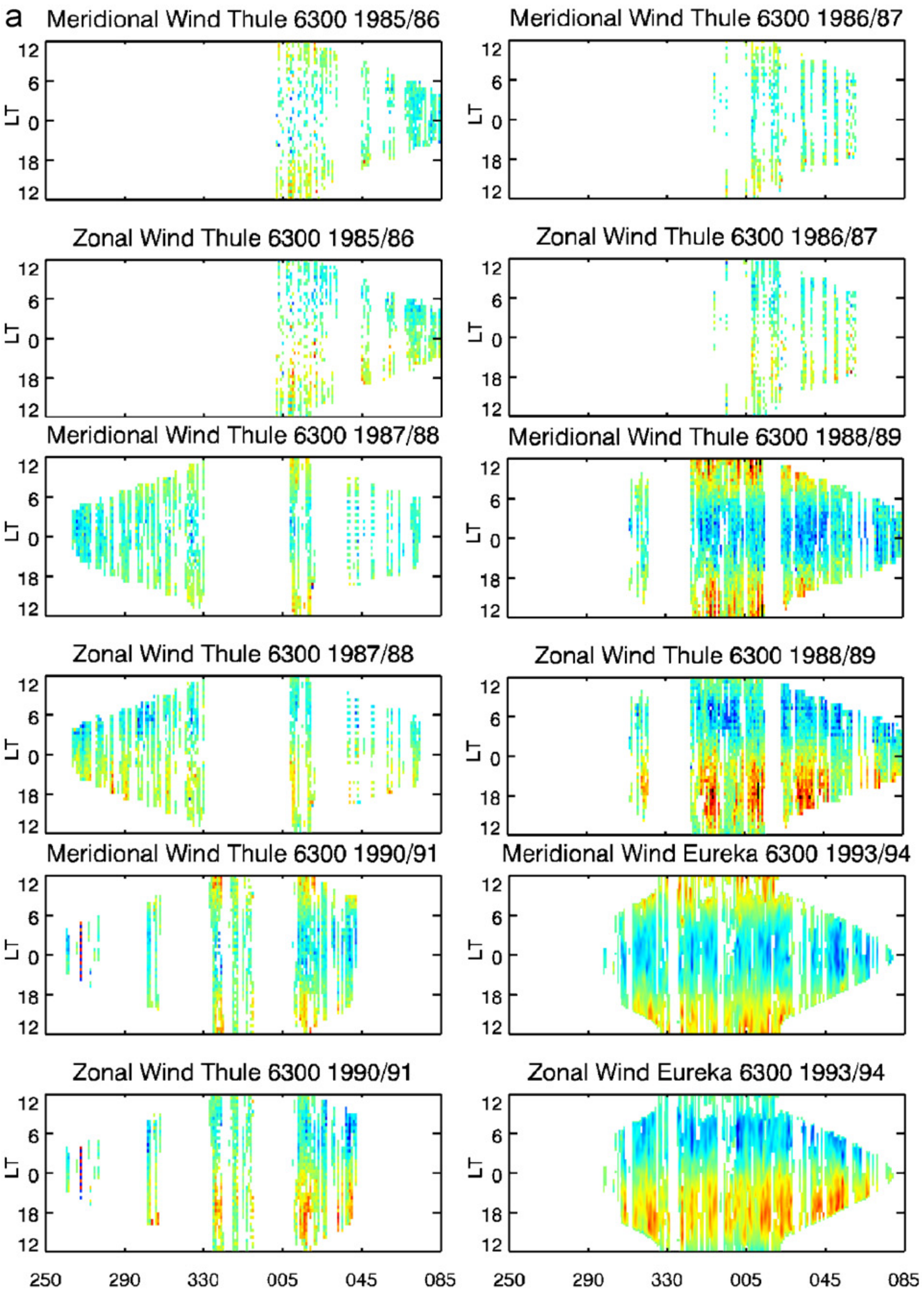

Fig. 3. Thule, Eureka, and Resolute neutral wind data survey plots. The data from different stations in different years are plotted in the same format. The Thermospheric wind meridional (upper panel) and zonal (lower panel) are shown in the plot. The local midnight is the middle of the each panel. The data coverage variation in local time is due to seasonal change of the length of nighttime in the northern polar region. Large data gaps are mostly due to instrumental problems. Short data gaps are weather related. Hourly cloud coverage data are used to remove data taken during cloudy sky.

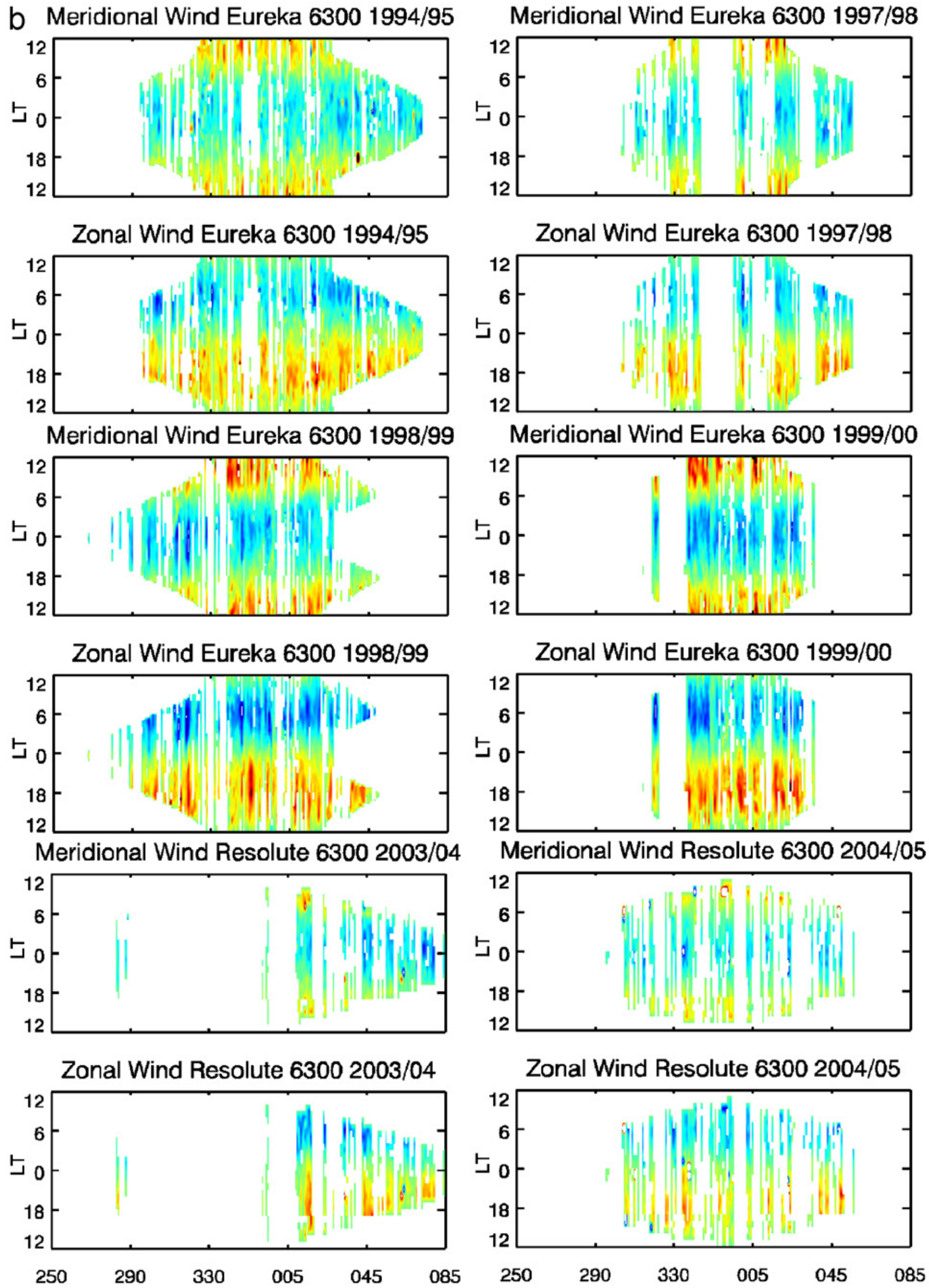

Fig. 3. (*Continued*)

In this paper, we used standard geomagnetic index driven TIEGCM runs based on the Heelis ion convection model (Heelis et al., 1982). The high-latitude cross-polar cap potential is K_p index driven with a formula, $CP = 15.+15 \times K_p+0.8 \times K_p^2$ (kV). We calculate the height-integrated model thermospheric winds using 6300 Å emission profiles, which are provided by the post-processor of the model. More information about TIEGCM output fields and model post-processors are available from the NCAR HAO web site (http://www.hao.ucar.edu/modeling/tgcm/tgcm.html).

The paper is organized as follows: In Section 2, we present observational results from Thule, Eureka, and Resolute. In Section 3, the TIEGCM results are compared with observations. Section 4 shows the derived diurnal and semidiurnal oscillations from TIEGCM and observations. We discuss our results in Section 5 and summarize our findings in Section 6.

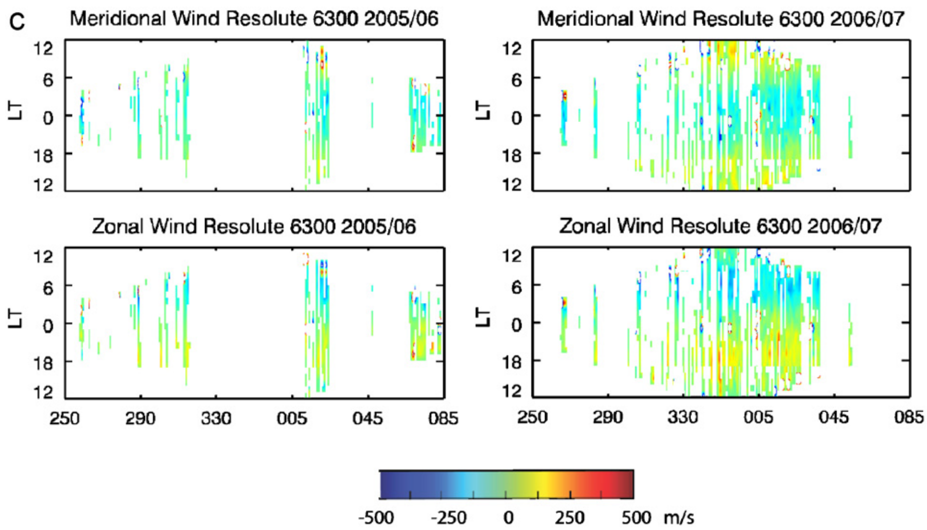

Fig. 3. (*Continued*)

2. Observations

2.1. Thule Observations

Thule FPI was located at the Thule Air Force Base in Greenland. The instrument had a pair 10.0 cm diameter etalon plates with a 12 channel image plane detector (Meriwether et al., 1988). The integration time was determined by the signal level of the nightglow ranging from 25 to 400 s. The instrument measured O 6300 Å neutral winds at the zenith and at four cardinal directions with an elevation angle of 45°. The wind error on average is about 13 m/s. The zero wind reference was obtained by averaging winds from all four cardinal directions. The horizontal winds were calculated assuming the horizontal winds are much greater than the vertical winds. Because of the long life time of the upper level of 6300 Å emission, the emission is strongly quenched at lower altitudes. Consequently, most of the emission comes from above 200 km and it peaks around 250 km. The wind measurements from ground-based optical instruments, of course, are height integrated. For better comparisons, the TIEGCM model results are also height integrated. More details about the instrument are provided by Meriwether et al. (1983). The instrument was operated at Thule from 1985/1986 winter season until 1990/1991 winter season. The survey plots of meridional and zonal wind data from 5 seasons are shown in Fig. 3. Data obtained during cloudy sky were removed. We used the hourly cloud cover data from local weather station in data selection. The criterion for data removal is cloud cover more than 50%. There was a clear trend of strong diurnal variations in both the meridional and zonal components. The local midnight is at the middle of the each panel and the local noon is on the upper and lower edge of the panel. The meridional wind had a minimum at midnight, meaning a negative (southward) wind and a maximum at the noon (northward winds). The diurnal variation in the zonal winds was off by 90° in phase from that of the meridional diurnal variations. This is a result of a mostly anti-sunward wind flow being reflected on meridional and zonal components. The data from the 1988/1989 winter season stranded out for stronger diurnal oscillations in both meridional and zonal components indicating a strong anti-sunward flow. The phase of this diurnal oscillation was roughly the same as that in the earlier winters.

2.2. Eureka observations

Eureka was the site of the Canadian Department of Environment ASTRO (Arctic STRatospheric Ozone observatory) laboratory. The Eureka FPI had a 15 cm diameter etalon with 20.5 mm spacing. The interferometer observation started in 1993/1994 winter season. The instrument took measurements at four cardinal directions at 25° elevation angle for the OH, O 5577 Å and O 6300 Å nightglow emissions. The instrument had an imaging photon detector until 1995. After 1995, the instrument used an intensified CCD detector to record the FPI fringes. The integration time for 6300 Å emission was 4 min. The entire multi-emission observation cycle took about 1 h. The wind error for the O 6300 Å emission was about 10 m/s. More information about the instrument is provided by Guo (2000). Fig. 3 shows Eureka data from 1993/1994 and 1999/2000 winter seasons with two winter seasons missing. The data showed consistently larger diurnal variation amplitude compared with the Thule data. The amplitudes were comparable with those of 1988/1989 winter season Thule data. The phase of the diurnal variation was the same as that in the Thule winds in local time.

2.3. Resolute observations

Resolute is the future site of the AMISR. A multi-emission FPI was deployed there in August 2003. This instrument samples neutral winds at vertical and four cardinal directions (45° elevation). The instrument has a 10 cm diameter etalon with a 2.0 cm gap. The etalon coating has 80% reflectivity at 6300 Å. The integration time is 5 min for the 6300 Å emission. The instrument also measures O 5577 Å and OH nightglow emissions. Because of multi-emission measurements, the entire observation cycle lasts about 1 h. Hence, we have two meridional (north and south) and zonal (east and west) wind component samples every hour, respectively. The wind error for the redline emission ranges from 2 to 6 m/s. The instrument has a SiTE 003 back-illuminated CCD with readout noise of 4 electrons. The data from 2003/2004 to 2006/2007 season are shown in Fig. 3. The diurnal variation amplitude was smaller than that of Thule data. The weather was not very favorable in Resolute compared with Thule and Eureka causing sparse data. Overall, the diurnal oscillation in the neutral winds at

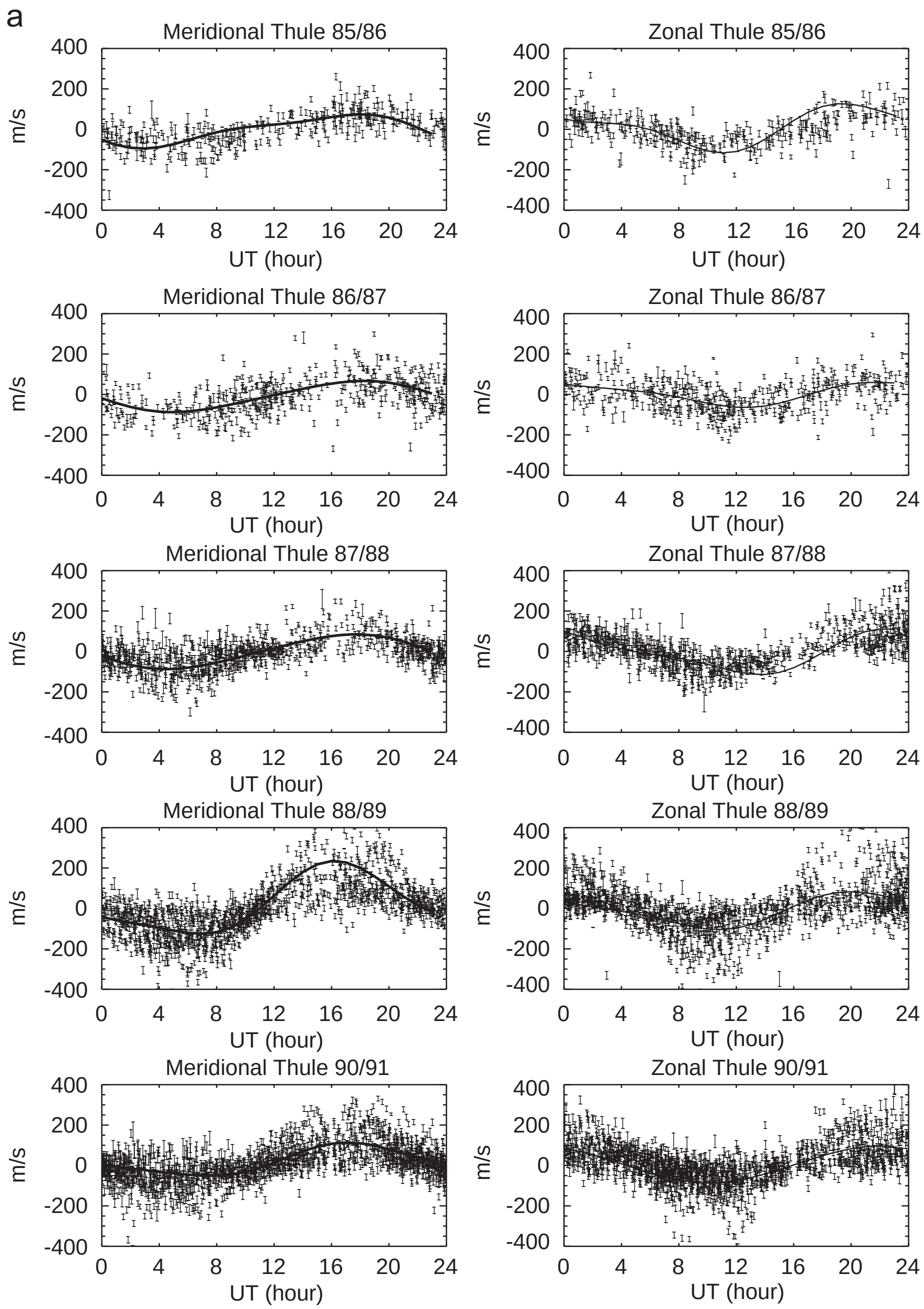

Fig. 4. Geomagnetic quiet time meridional and zonal wind data and least squares fit results. The left (right) side is for the meridional (zonal) component. Data from all available years are plotted and analyzed. The meridional and zonal wind data are selected when the sky condition is clear and K_p is less than 2.

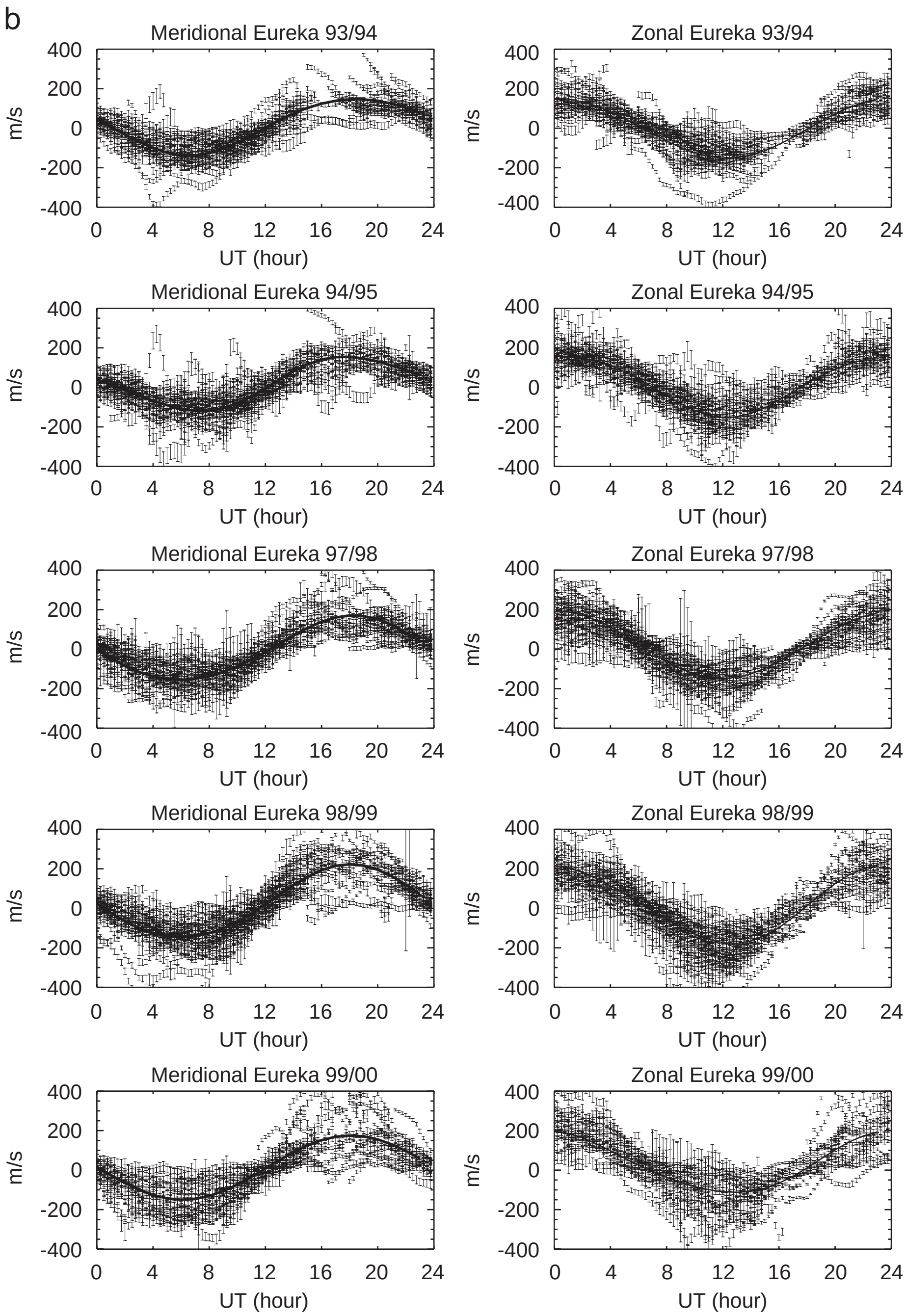

Fig. 4. (*Continued*)

Resolute appeared to be smaller than that at Eureka and Thule.

2.4. Analysis of thermospheric winds

By examining the survey plots of data from all stations, we noted large inter-annual variations and inter-station differences. To quantify these variations and differences, we performed least squares fit to the all data from day 250 to day 84 of all winter seasons under clear weather condition and $K_p < 2$. That time interval covers the winter season for each station as shown in earlier survey plots (Fig. 3). The selection of data of low geomagnetic activity ensures that the geomagnetic effect is not a major factor in the final results. The least squares fitting curves and observational data are plotted in Fig. 4. The least squares fit curve consist a background wind (time-constant wind), diurnal and semidiurnal oscillations. The fitting is performed for both the meridional and zonal wind components.

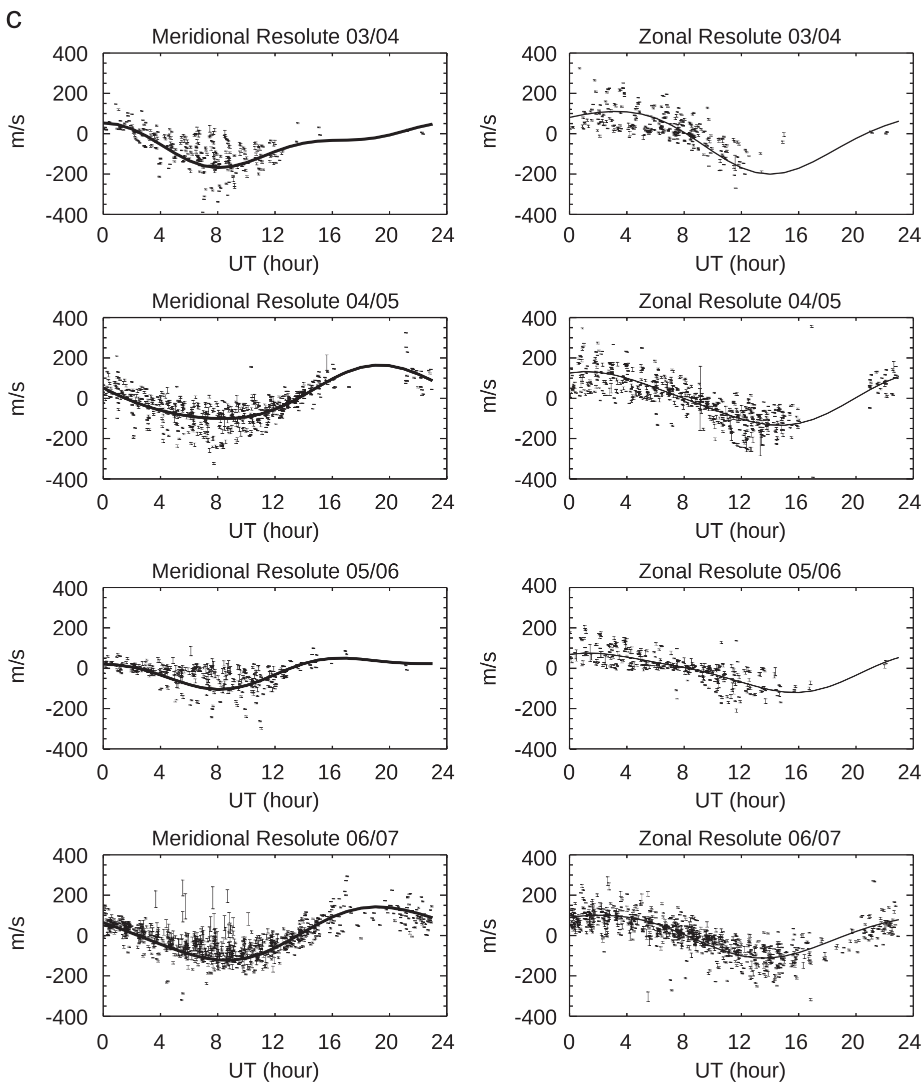

Fig. 4. (*Continued*)

The Thule data had fairly good local time coverage from midnight to noon. The Eureka data coverage was even better due to good weather conditions. The Resolute coverage was relatively sparse due to unfavorable weather condition. The coverage near-local noon was mostly absent due to the lower latitude location of the station compared with other two stations. At lower latitudes the Sun is not far from the horizon during the local noon. The lack of coverage near-local noon during 2003/2004 winter season might impact the least squares fitting results. The results of the fitting are plotted in Fig. 10 along with the TIEGCM result.

3. NCAR-TIEGCM run and observation comparison

To investigate further the inter-station differences and solar dependence, we used NCAR-TIEGCM model for 10-day run centered at the December solstice for the years of 1985, 1988, 1994, 1999, 2003, 2004, 2005, and 2006. The model runs can provide some explanation for our observations over the last 20 years. For those years, in which we have good solstice coverage, we plot a detailed comparison between the model output and the observations. During the December solstice, the FPI data usually have 24 h coverage, weather permitting. Fig. 5 shows the comparison between the TIEGCM run and the Thule observations during the 1988 December solstice. The TIEGCM winds are height integrated based on the 6300 Å emission profiles in the model post-processor. The goal is to reduce model-data discrepancy may arise from the height integration effect in the neutral wind measurements The TIEGCM and FPI winds show a good agreement in the zonal direction. The TIEGCM meridional winds tend to have larger diurnal variations than that of FPI observations. Mainly due to larger meridional wind variations, the simulated TIEGCM wind magnitudes are larger than those observed by the FPI.

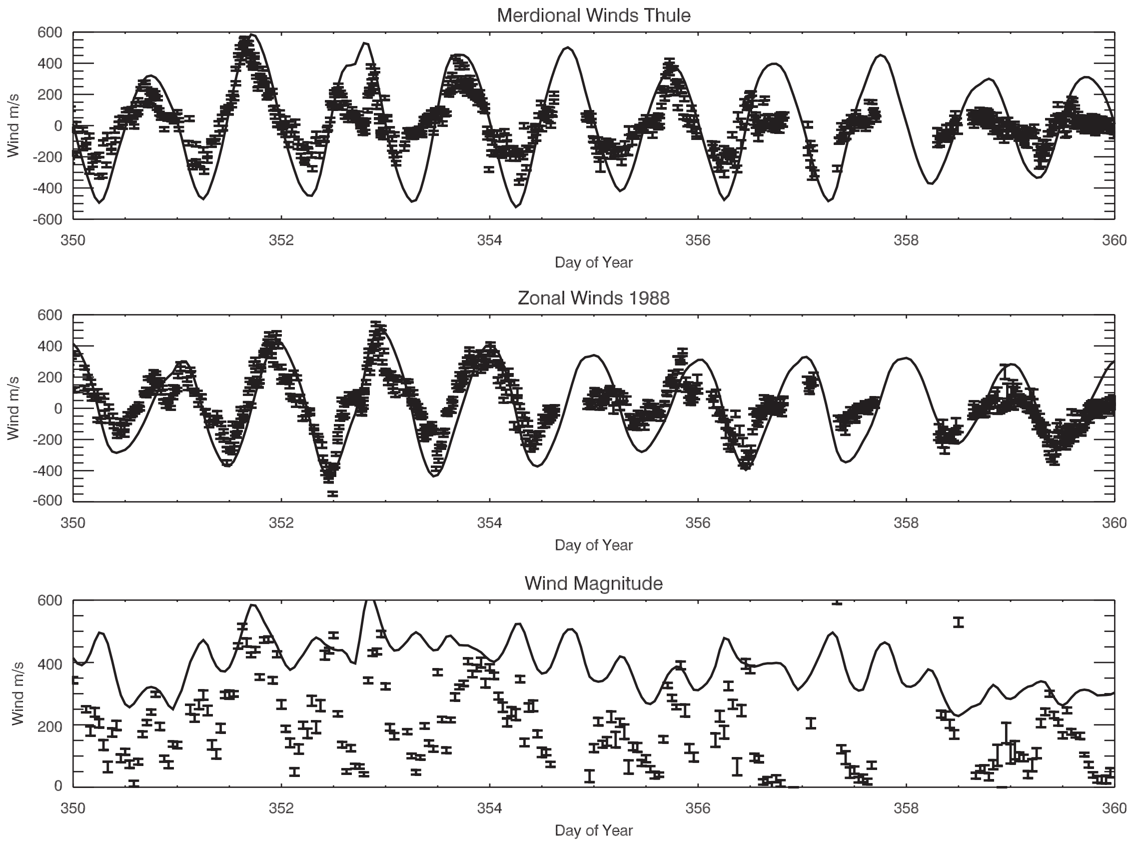

Fig. 5. TIEGCM and Thule 1988 comparison. TIEGCM Thermospheric winds from height integration with 6300 Å emission profile are plotted (line). The observations from Fabry–Perot interferometer are plotted with error bars. The meridional (top), zonal (middle) and magnitude (lower) are shown in three panels. Data gaps are mostly due to cloudy sky condition.

Fig. 6 plots the winds from the Eureka 1994 data and compares them with TIEGCM run results. Again, the meridional winds tend to have large discrepancies than zonal winds. The agreement in zonal winds is quite remarkable. The TIEGCM tends to predict larger southward winds. The observed wind magnitudes are also smaller than the TIEGCM run results. Fig. 7 shows the 1999 Eureka data comparison with the TIEGCM run. In this case, the meridional and zonal winds show similar agreements between observations and model. Observations tend to show smaller westward peaks in zonal winds than those from the simulation.

Fig. 8 is for the Resolute 2004 winter season. Wind variations were smaller in both meridional and zonal components compared with Thule and Eureka. Wind magnitudes were also smaller. In general, the agreement is better between the TIEGCM simulations and FPI observations in the zonal direction than in the meridional direction. Fig. 9 is for the 2006 winter season at Resolute. The results were similar to that of the 2004. The meridional winds show large discrepancies between the TIEGCM and FPI observations, but the agreement for the zonal component is excellent. Wind magnitudes from the TIEGCM are in general larger than that observed by the FPI.

4. Analysis result comparisons

Fig. 10 shows the least square fitting results from the observational data at all stations for each of the winter seasons. Using the TIEGCM simulation results for the 10 days centered at winter solstice, we select the simulation data under the condition of $K_p<2$. Then we perform the same least squares fit to the selected TIEGCM data to extract the background wind, diurnal, and semidiurnal oscillations for comparison with the observation. We should note that the TIEGCM selection is from the 10-day interval near the winter solstice, whereas the observation selection is from a much longer interval (200-day, not all have full 24-h coverage). We also plotted mean F10.7 index for all winters under good weather conditions when observations were made in Fig. 10 for reference.

4.1. Diurnal oscillation

The amplitude in the meridional wind from Thule showed a sharp increase in 1988/1989 winter season, while that of the zonal component did not. A closer examination of the zonal wind data in 1988/1989 in Fig. 4 showed an increase in diurnal oscillation in some data

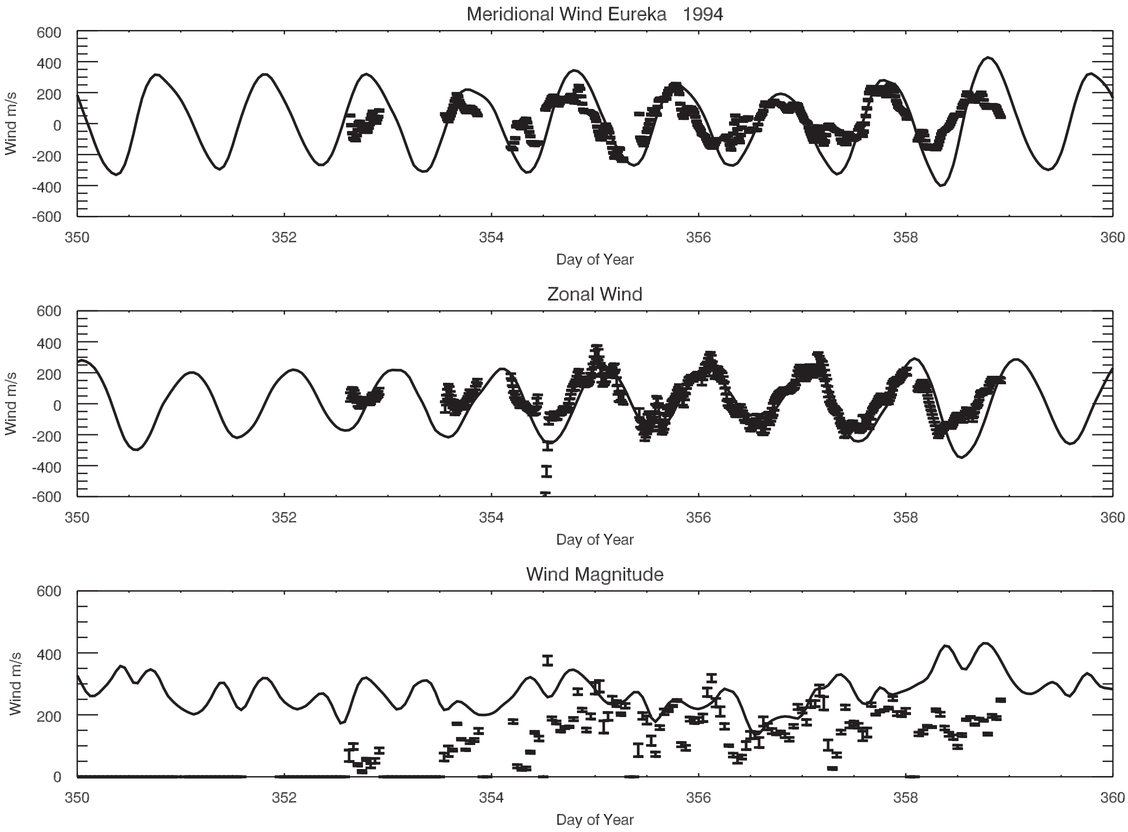

Fig. 6. TIEGCM and Eureka 1994 comparison. Same as Fig. 5 for Eureka 1994.

points, however, that was not enough to alter the results of the least squares fitting results. The 1988/1989 peak in the meridional wind coincided with the solar maximum in the same year. The Eureka data showed persistently high diurnal oscillation levels in both the meridional and zonal components compared with the Thule results. We see a slight increase in 1998/1999 winter season. The Resolute data showed smaller amplitudes than those at Eureka. Most of the meridional amplitude is similar to that of the zonal amplitude. There appeared to be a minimum during year 2005/2006, when the solar F10.7 index also reached bottom.

The amplitudes from the TIEGCM simulation show larger meridional oscillations than that of zonal oscillation (the thin solid-lines are higher than the dashed-lines). The oscillations at the Thule and Eureka (red and blue lines) are larger than these at the Resolute (green lines) according to the TIEGCM simulation (blue- and red-lines are higher than the green-line). The oscillation amplitudes at Thule and Eureka are very similar. This is true for both meridional and zonal components. We also see a larger peak in 1988/1989 winter than that in 1999/2000 winter.

The TIEGCM simulation shows stronger oscillations than those from observation in general and particularly for the meridional component (solid-lines). For Resolute the simulated TIEGCM amplitudes are comparable to those from the observation.

The observed phase of the meridional oscillation showed an approximately 1-h shift from Thule to Eureka and to Resolute in UT. That is consistent with the local time shift for the three stations. Large deviations from this trend occurred during 1985/1986 and 2003/2004 winter seasons. During the 2003/2004 winter season, the absence of data in a large local time section (12–24 UT) could be the cause of the large discrepancy. The TIEGCM results also show a roughly 1-h phase shift from Thule to Eureka and to Resolute in UT. However, the TIEGCM show a 1-h phase difference from the observations. That is consistent with the comparison shown in Figs. 6–9, in which the oscillation in data have a tendency to lead that in the model results. Both the observation and simulation results display an approximately 6-h phase offset between the meridional and zonal component, which is an evidence of wind vector rotation.

The observed phase of the oscillation in the zonal direction shows large jumps at Thule (blue dotted-line), while the phase at other stations remain mostly stable. At Eureka the observed phase of the zonal wind diurnal oscillation (red dotted-line) is shifted by 1-h from the TIEGCM prediction (red dashed-line). At Resolute the observed phase agree with the TIEGCM prediction very well. Unlike that in the meridional winds, the zonal wind diurnal oscillation phase from the TIEGCM shows no phase shift between Eureka and

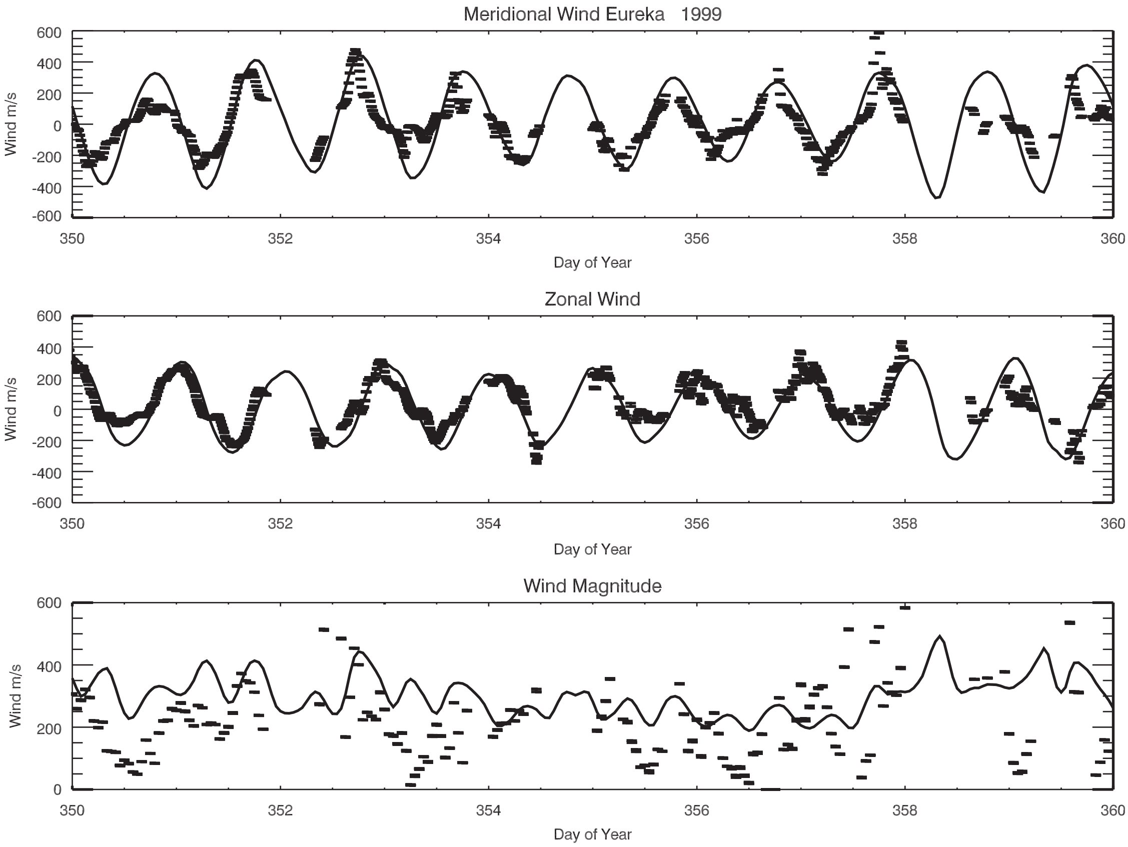

Fig. 7. TIEGCM and Eureka 1999 comparison. Same as Fig. 5 for Eureka 1999.

Resolute, whereas the observation showed about 1-h phase difference.

4.2. Semidiurnal oscillation

The observed meridional and zonal amplitudes showed large fluctuations at Thule. The observed meridional and zonal oscillations at Eureka have small fluctuations and did not have the large values shown at Thule. The amplitudes in two wind components (thick green dotted- and solid-lines) at Resolute were greater than that at Eureka. Large semidiurnal amplitude in 2003/2004 at Resolute was seen in the meridional winds. For the most part, the semidiurnal oscillation at Resolute did not change much in meridional and zonal winds over these three winter seasons.

The TIEGCM results show relatively small variations in the amplitude at Resolute and Eureka during all winters in meridional winds (thin red and green solid-lines). The Resolute results have consistently larger amplitudes than those from Eureka and Thule. The Thule TIEGCM meridional results showed large jumps. Overall, they are smaller than Resolute and Eureka results. The TIEGCM zonal results (dashed-lines) show larger amplitudes at Thule and Resolute and smaller values at Eureka. In general the zonal oscillation is smaller than that in the meridional component in the TIEGCM simulation.

The TIEGCM simulation of the semidiurnal oscillation is consistent with observation in two aspects: (1) resolute has larger amplitudes than Eureka in both the meridional and zonal components; (2) the TIEGCM zonal semidiurnal oscillation amplitudes are comparable with those from the FPI observations.

The phases of TIEGCM show similar time shifts from Resolute to Eureka, and to Thule. The phase at Thule leads other two stations, which is in line with the local times of each of the stations. The TIEGCM also shows consistent nearly 3-h off set between the meridional and zonal winds (90°) indicating the semidiurnal oscillation is also a rotating oscillation like the diurnal oscillation. Such consistent meridional and zonal component phase offset is not evident for all winters from observational results.

4.3. Background winds (time-constant winds)

Most of the background winds values (meridional and zonal) are limited to a range from -20 to 30 m/s for both the simulation and observations. The exception is the winter 2003/2004 observation at Resolute, where large negative values were obtained from the least squares

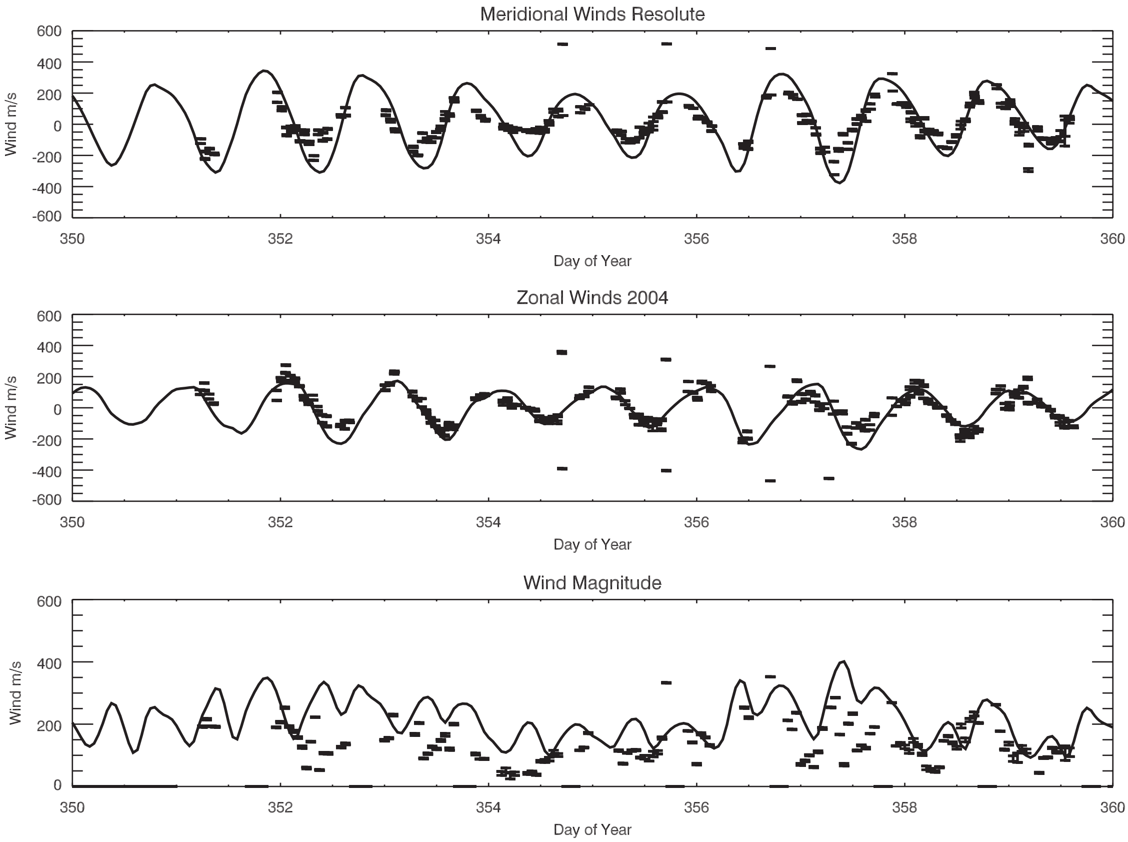

Fig. 8. TIEGCM and Resolute 2004 comparison. Same as Fig. 5 for Resolute 2004.

fitting. Given the large data gap from 12 to 24 UT during that observational season, we can expect some bias in the fitting results. The TIEGCM simulation shows a larger meridional background winds at Resolute for all years and followed by Eureka (thin green and red solid-lines). For the zonal component, we see larger background winds at Thule, followed by Eureka and Resolute (thin dashed-lines). Observational results appeared to show slightly large backgrounds at Eureka for both the meridional and zonal components. This is consistent with the TIEGCM simulation for the zonal component.

4.4. Diurnal oscillation and F10.7 index

To examine the correlation between the amplitude of the diurnal oscillation (in meridional and zonal winds) and F10.7 index, we plot one parameter vs another in Fig. 11. The distribution of the data points from each stations show varying degrees of correlation between the two parameters. The Thule station (blue) had large ranges of the F10.7 index values and diurnal oscillation amplitudes. Correlation between the two parameters is clearer for the meridional winds (blue triangles) than that of the zonal winds (blue diamonds). The Eureka data distribution was more compact. An offset towards high diurnal oscillation amplitude for Eureka is apparent. Correlation between diurnal oscillation amplitude and F10.7 index was similar to that of Thule within the small range of the F10.7 index values. The Resolute data congregated in an even smaller area. Because of limited range of the F10.7 index values, it will be difficult to assess the correlation between the two parameters for Resolute data. More data are needed to see if the sharp increase in diurnal oscillation amplitude with the F10.7 index is real or not.

5. Discussion

There is no doubt that high-latitude thermospheric winds are affected by the solar activity due to changes in the thermosphere temperatures and thus pressure gradients. However, just how the thermospheric wind at high latitudes is connected to the solar activity was not precisely known. Current knowledge is based on mostly the Thule data set alone. In this study, we added Eureka and Resolute data. Based on the Eureka and Thule data sets we can see an indication of correlation between the diurnal oscillation amplitudes in the meridional component and the F10.7 index. However, when we combine all data together, we also notice significant inter-station differences. We suspect that the cause for the difference is because Eureka is located at higher magnetic latitude than both Thule and Resolute. At higher magnetic latitude, the station is in the fast anti-sunward transpolar flow conver-

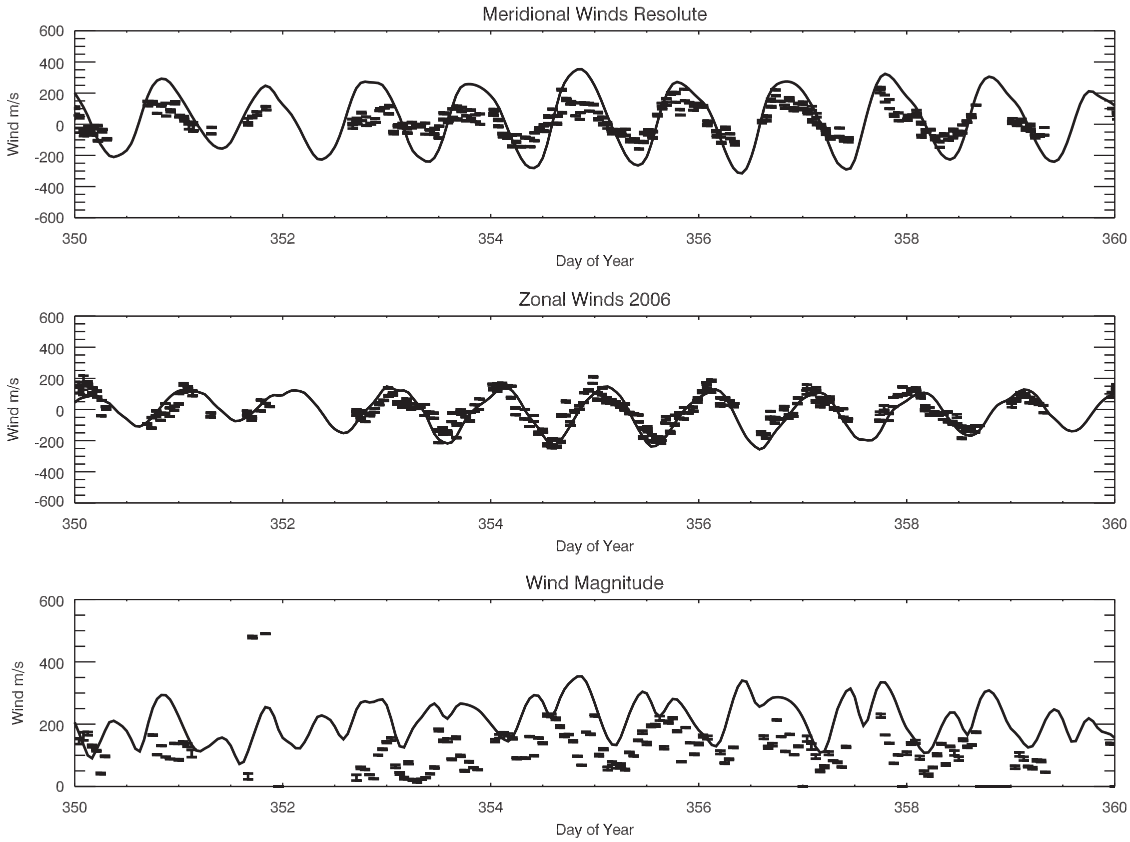

Fig. 9. TIEGCM and Resolute 2006 comparison. Same as Fig. 5 for Resolute 2006.

ging area of two-cell convection pattern during most local times. That leads to a stronger anti-sunward wind and stronger diurnal oscillations in meridional and zonal components at Eureka. Thule and Resolute, on the other hand, are nearer the centers of the convection cells on the dawn and dusk sides. The wind magnitudes at the centers of convection cells are smaller, which reduces the wind magnitude overall. On the other hand, because Resolute passes the convection cell centers at dawn and dusk, the Resolute data should see a stronger semidiurnal oscillation. Conversely, the semidiurnal oscillation is small at Eureka, because it is far away from the convection cell centers.

To investigate the inter-station and solar dependence of the thermospheric winds, we use the NCAR-TIEGCM 1.8 model to simulate thermospheric winds at three stations during the December solstice period for several years spread out during the 20-year period. The comparison for each individual station shows a very good agreement in the zonal winds between the simulation and observation. The simulation also showed large inter-station differences between Resolute and the other two stations, Eureka and Thule in terms of meridional and zonal diurnal oscillations. The simulation showed very small differences between Thule and Eureka. Such inter-station differences are not quite same as we observed. Given the 5° grid size of the TIEGCM, it may not be able to fully resolve the inter-station difference between Thule and Eureka. In fact, Thule and Eureka all fall into the same geographic latitudinal grid centered at 77.5°N while Resolute belongs to the grid at 72.5°N. The model is correct in showing a relatively small diurnal oscillation in thermospheric winds at Resolute. Hence, the model appears to confirm the cause of the inter-station differences is due to difference in magnetic latitude.

On the semidiurnal oscillation, the TIEGCM predicts larger amplitudes at Resolute than that at the Eureka as shown by observations, as we have explained earlier due to Resolute passing the centers of convection cells. The simulation at Thule is not consistent with observations. Observations show larger semidiurnal oscillation at Thule than that at Eureka, whereas the TIEGCM predicts the opposite.

The TIEGCM consistently predicts larger meridional diurnal and semidiurnal oscillations than those observed at the three stations. That could be because to the forcing used in the model is more than what is needed. Future adjustments in the model are under consideration.

Because we do not have a cross calibration between the three instruments at the same location and same time, we cannot rule out completely some systematic instrumental differences. Given that the principle of the FPI measurement is well known and data processing is not model dependent, such instrument differences should be very small. Furthermore, we know that potential sources for

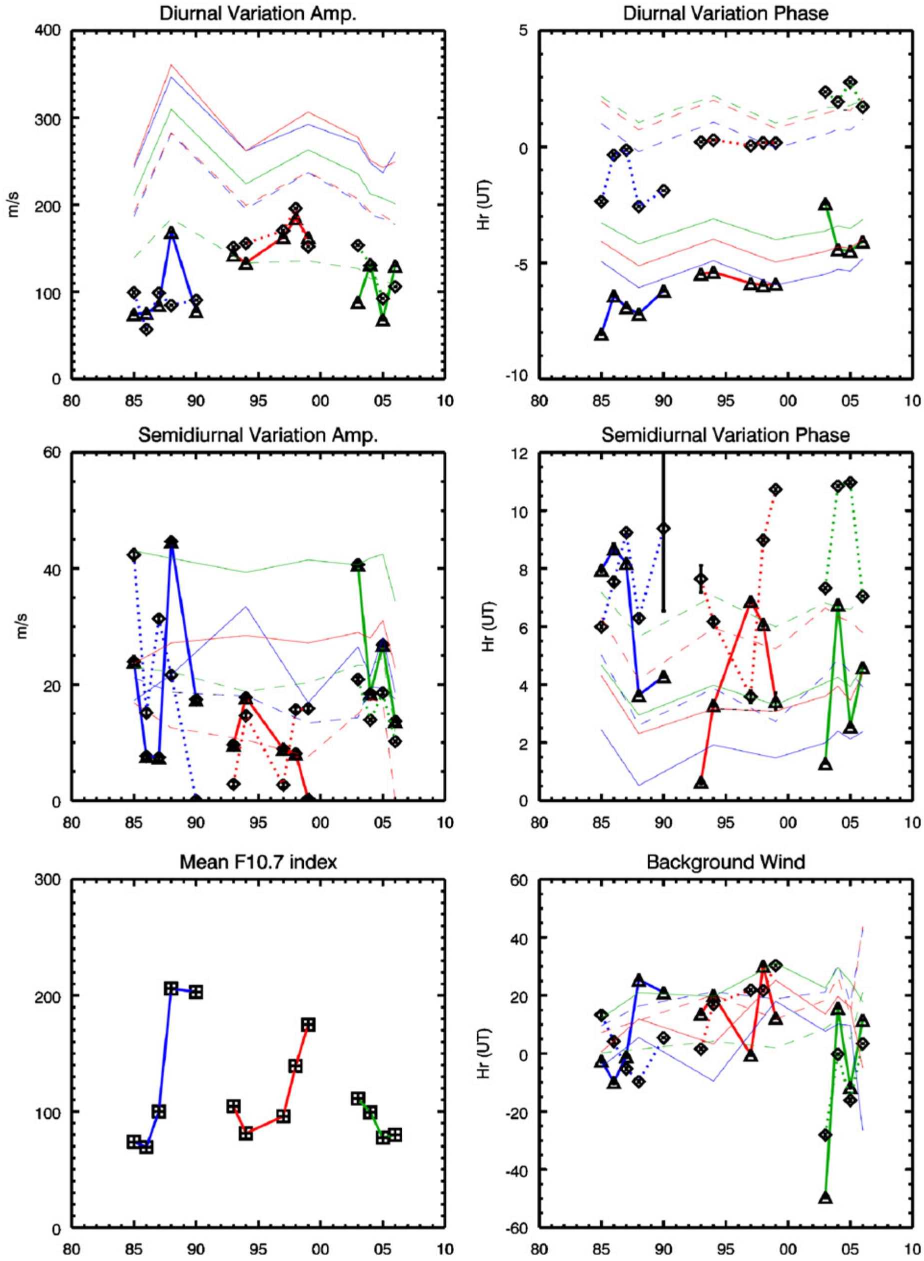

Fig. 10. Thermospheric wind analysis results and comparison with model output. The least squares fit results of the observations and model simulations. The Thule (blue), Eureka (red), and Resolute (Green) results are plotted in the figure. The triangles linked with thick solid-lines are from the meridional wind observational results. The diamonds linked with thick dotted-lines are from the zonal wind observational results. The thin solid-lines (dashed-lines) are from the meridional (zonal) wind of TIEGCM simulation results for winter solstice of years 85, 88, 94, 99, 03, 04, 05, and 06.

systematic errors are errors in etalon gap and focal length of the focusing lens, which are all determined to very high accuracies. Hence, we do not see an obvious cause for systematic errors in the instruments at this moment. But it is curious to note that the inter-station differences from the TIEGCM are mostly consistent for Eureka and Resolute in terms of the amplitudes of the diurnal and semidiurnal oscillations and inconsistent with the Thule observations. To fully resolve this issue, simultaneous observations at these three stations are needed.

6. Summary

We examined the solar dependences of the thermosphere dynamics based on 20-year observations of polar cap thermospheric winds. The strong diurnal oscillations in meridional and zonal components are a reflection of anti-sunward wind. We summarize our results: (1) we see a clear association between the meridional diurnal oscillation in the thermospheric wind and the F10.7 index in both observation and simulation; (2) the TIEGCM

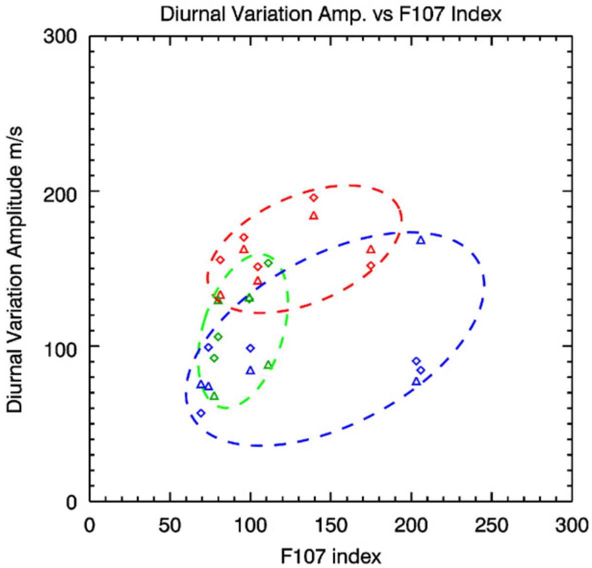

Fig. 11. Diurnal oscillation vs. F10.7 index. The meridional (triangles) and zonal (diamonds) diurnal oscillations from Thule (blue), Eureka (red), and Resolute (green) are plotted against the averaged F10.7 index values shown in Fig. 10. The dashed lines mark the rough boundaries of data point distributions from each station.

simulated Resolute and Eureka inter-station differences are mostly consistent with observation; (3) the diurnal oscillation at Eureka is stronger than that at Resolute according to both observation and simulation; (4) the semidiurnal oscillation at Resolute is stronger than that at Eureka based on data and model results; and (5) the simulated meridional diurnal and semidiurnal oscillations are stronger than what was observed and future adjustments to the model are under consideration.

With the future deployment of AMISR, we anticipate the combined observations of the thermospheric winds and ion drift will shed more light on high-latitude thermosphere and ionosphere coupling and the magnetosphere influence on the polar cap ionosphere. Due to the complex nature of the high-latitude thermospheric wind convection, it is highly desirable to have simultaneous observations from these three stations and higher resolution simulations from the TIEGCM in the future.

Acknowledgments

The Resolute Fabry–Perot interferometer operation and analysis is supported by a grant from the National Science Foundation ATM 0334595. The Resolute Early Polar Cap Observatory is operated and managed by SRI International with funding from the National Science Foundation's Upper Atmospheric Facilities Program. The National Center for Atmospheric Research is sponsored by the National Science Foundation. The Eureka observatory is operated by the Atmospheric Environment Service of Canada. The Thule operation was supported by both the National Science Foundation and Air Force to the University of Michigan. Authors would like to thank Prof. J. Meriwether and Dr. Killeen for their effort in the FPI operation in Thule. We would like to thank two referees for their suggestions and comments. Dr. Alan Burns also provided many suggestions.

References

Aruliah, A.L., Rees, D., Steen, A., 1991. Seasonal and solar-cycle variations in the high latitude thermospheric winds. Geophysical Research Letters 18, 1983–1986.

Aruliah, A.L., Farmer, A.D., Rees, D., 1996. The seasonal behavior of high-latitude thermospheric winds and ion velocities observed over one solar cycle. Journal of Geophysical Research 101, 15701–15711.

Conde, M., Dyson, P.L., 1995. Thermospheric horizontal winds above Mawson, Antarctica. Advances in Space Research 16, (5)41–(5)52.

Emmert, J.T., Faivre, M.L., Hernandez, G., Jarvis, M.J., Meriwether, J.W., Niciejewski, R.J., Sipler, D.P., Tepley, C.A., 2006a. Climatologies, of nighttime upper thermospheric winds measured by ground-based Fabry–Perot interferometers during geomagnetically quiet conditions 1. Local time, latitudinal, seasonal, and solar cycle dependence. Journal of Geophysical Research 111, A12302.

Emmert, J.T., Hernandez, G., Jarvis, M.J., Meriwether, J.W., Niciejewski, R.J., Sipler, D.P., Vennerstrom, S., 2006b. Climatologies, of nighttime upper thermospheric winds measured by ground-based Fabry–Perot interferometers during geomagnetically quiet conditions 2. High latitude circulation and interplanetary magnetic field dependence. Journal of Geophysical Research 111, A12303.

Greet, P.A., Conde, M.G., Dyson, P.L., Innis, J.L., Breed, A.M., 1999. Thermospheric wind field over Mawson and Davis Antarctica; simultaneous observations by two Fabry–Perot spectrometers of λ 630 nm emission. Journal of Atmospheric Solar-Terrestrial Physics 61, 1025–1045.

Guo, W., 2000. F-region winds over the central polar cap. Ph.D. Thesis, University of Saskatchewan, Saskatoon.

Heelis, R.A., Lowell, J.K., Spiro, R.W., 1982. A model of the high-latitutde ionosphere convection pattern. Journal of Geophysical Research 87, 6339–6345.

Heelis, R.A., McEwen, D., Guo, W., 2002. Ion and neutral motions observed in the winter polar upper atmosphere. Journal of Geophysical Research 107.

Hernandez, G., Roble, R.G., 2003. simultaneous thermospheric observations during the geomagnetic storm of April 2002 from South Pole and arrival heights, Antarctica. Geophysical Research Letters 30, 1511.

Hernandez, G., McCormac, F.G., Smith, R.W., 1991. Austral thermospheric wind circulation and interplanetary magnetic field orientation. Journal of Geophysical Research 96, 5777–5783.

Hernandez, G., Smith, R.W., Roble, R.G., Gress, J., Clark, K.C., 1990. Thermospheric dynamics at the South Pole. Geophysical Research Letters 17, 1255–1258.

Killeen, T.L., Heelis, R.A., Hays, P.B., Spencer, N.W., Hanson, W.B., 1985. Neutral motions in the polar thermosphere for northward interplanetary magnetic field. Geophysical Research Letters 12, 159–162.

Killeen, T.L., Won, Y.-I., Niciejewski, R.J., Burns, A.G., 1995. Upper thermospheric winds and temperatures in the geomagnetic polar cap: solar cycle, geomagnetic activity, and interplanetary magnetic field dependencies. Journal of Geophysical Research 100, 21327–21342.

McCormac, F.G., Smith, R.W., 1984. The influence of the interplanetary magnetic field *Y*-component on the ion and neutral motions in the polar thermosphere. Geophysical Research Letters 11, 935–938.

McCormac, F.G., Killeen, T.L., Gombosi, E., Hays, P.B., Spencer, N.W., 1985. Configuration of the high-latitude thermosphere neutral circulation for IMF By negative and positive. Geophysical Research Letters 12, 155–158.

Meriwether, J.W., Tepley, C.A., Price, S.A., Hays, P.B., Cogger, L.L., 1983. Remote ground-based observations of terrestrial airglow emissions and thermospheric dynamics at Calgary, Alberta, Canada. Optical Engineering 22, 128–131.

Meriwether, J.W., Killeen, T.L., McCormac, F.G., Burns, A.G., 1988. Thermospheric winds in the geomagnetic polar cap for solar minimum conditions. Journal of Geophysical Research 93, 7478–7492.

Niciejewski, R.J., Killeen, T.L., Won, Y., 1994. Observations of neutral winds in the polar cap during northward IMF. Journal of Atmospheric Terrestrial Physics 56, 285–295.

Richmond, A.D., Ridley, E.C., Roble, R.G., 1992. A thermosphere/ionosphere general circulation model with coupled electrodynamics. Geophysical Research Letters 19, 601–604.

Smith, R.W., Hernandez, G., Price, K., Fraser, G., Clark, K.C., Schulz, W.J., Smith, S., 1994. The June 1991 thermospheric storm observed in the Southern hemisphere. Journal of Geophysical Research 98, 17609–17615.

Thayer, J.P., Crowley, G., Niciejewski, R.J., Killeen, T.L., Buchau, J., Reinisch, B.W., 1995. Ground-based observations of ion/neutral coupling at Thule and Qanaq, Greenland. Journal of Geophysical Research 100, 12189–12199.

Witasse, O., Lilensten, J., Lathuilere, C., Pibaret, B., 1998. Meridional thermospheric neutral wind at high latitude over a full solar cycle. Annales Geophysicae 16, 1400–1409.

Won, Y.-L., 1994. Studies of thermospheric neutral winds utilizing ground-based optical and radar measurements, Ph.D. Thesis, University of Michigan, Ann Arbor.